



LAWRENCE
LIVERMORE
NATIONAL
LABORATORY

Absolute determination of charge-coupled device quantum detection efficiency using Si K-edge x-ray absorption fine structure

J. Dunn, A. B. Steel

May 8, 2012

High Temperature Plasma Diagnostics 2012
Monterey, CA, United States
May 7, 2012 through May 10, 2012

Disclaimer

This document was prepared as an account of work sponsored by an agency of the United States government. Neither the United States government nor Lawrence Livermore National Security, LLC, nor any of their employees makes any warranty, expressed or implied, or assumes any legal liability or responsibility for the accuracy, completeness, or usefulness of any information, apparatus, product, or process disclosed, or represents that its use would not infringe privately owned rights. Reference herein to any specific commercial product, process, or service by trade name, trademark, manufacturer, or otherwise does not necessarily constitute or imply its endorsement, recommendation, or favoring by the United States government or Lawrence Livermore National Security, LLC. The views and opinions of authors expressed herein do not necessarily state or reflect those of the United States government or Lawrence Livermore National Security, LLC, and shall not be used for advertising or product endorsement purposes.

Absolute determination of charge-coupled device quantum detection efficiency using Si K-edge x-ray absorption fine structure^{a)}

J. Dunn,^{1,b)} and A. B. Steel^{1,2}

¹*Lawrence Livermore National Laboratory, P.O. Box 808, Livermore, California 94550, USA*

²*Department of Applied Sciences, University of California, Davis, California 95616, USA*

(Presented XXXXX; received XXXXX; accepted XXXXX; published online XXXXX)

We report a method to determine the quantum detection efficiency and the absorbing layers on a front-illuminated charge-coupled device (CCD). The CCD under study, as part of a crystal spectrometer, measures intense continuum x-ray emission from a picosecond laser-produced plasma and spectrally resolves the Si K-edge x-ray absorption fine structure features due to the electrode gate structure of the device. The CCD response across the Si K-edge shows a large discontinuity as well as a number of oscillations that are identified individually and uniquely from Si, SiO₂, and Si₃N₄ layers. From the spectral analysis of the structure and K-edge discontinuity, the active layer thickness and the different absorbing layers thickness can be determined precisely. A precise CCD detection model from 0.2 – 10 keV can be deduced from this highly sensitive technique.

I. INTRODUCTION

The quantum detection efficiency (QDE) of charge-coupled devices (CCD) to soft x-rays depends critically on the photon energy, the device active thickness (epitaxial layer) and the surface layers in front-illuminated (FI) or back-illuminated (BI) architecture.^{1,2} The measurement of plasma x-ray emissivity with spectroscopic instrumentation requires precise determination of the QDE and these absorbing layers in particular. For FI devices, the x-rays have to transverse the electrode gate structure consisting of absorbing layers of various chemical compositions (Si, SiO₂, Si₃N₄) typically about 1 μm thick. For the BI devices, the backside of the detector is thinned, substantially reducing the effect of the residual dead layer absorption (Si, SiO₂) and allowing higher detection efficiency useful below 1 keV. In either case, there is a very strong effect in the QDE above 1 keV and in particular around the Si K-edge at 1.84 keV depending on the device architecture.^{1,3} Precise determination of the absorbing layers and corresponding coefficients is therefore important. Detailed studies using synchrotron sources have provided a precise data set of the photo-absorption coefficients and x-ray absorption fine structure (XAFS) over the Si K-edge for known thicknesses of Si-composed layers.^{3,4} CCD detection models have been constructed and compared with experimental measurements. The detection efficiency of CCDs and other solid-state detectors can be determined over different energy ranges using monochromatic synchrotron sources³, calibrated hard K α x-ray tubes,^{5,6} or laser plasma sources producing a soft x-ray continuum over the Si L-edge reported for a back-illuminated device.²

We report another method to determine the QDE and the absorbing layers: A CCD-based crystal spectrometer measuring intense continuum x-ray emission from a picosecond laser-produced plasma clearly shows the Si K-edge XAFS features in the spectrum due to the gate structure of the FI device. The CCD response across the Si K-edge shows a large discontinuity as well as a number of oscillations that are distinctly identified as from Si, SiO₂, and Si₃N₄ layers. From the analysis of the XAFS and K-

edge discontinuity in the spectrum, the active layer thickness of the device is determined precisely. In addition, the different absorbing layers thicknesses are determined. The main conclusion of this study reports that a precise CCD detection model over a wide energy range (0.2 – 10 keV) can be deduced by measuring the detector Si K-edge response over a narrow x-ray energy band centered at 1.84 keV.

II. EXPERIMENTAL DESCRIPTION

A flat crystal spectrometer using a Potassium Hydrogen Phthalate KAP (100), $2d = 26.632\text{\AA}$, crystal and a CCD detector was fielded on the short pulse Jupiter Laser Facility Titan at the Lawrence Livermore National Laboratory. The spectrometer was used to record spectra of 1.5 – 2.5 keV x-rays from various laser-produced plasmas of low Z foils and CH-coated, buried layer targets as part of a dense plasma study. The instrument was operated at shallow Bragg angles in the range of 10 – 17° with the spectrometer viewing through the back of the target. The x-ray path from detector to source distance via the crystal was 27.3cm. The short pulse laser was incident on the front at 45° to target normal with parameters of 20 – 50 J at 527 nm wavelength energy on target, 0.7 ps (FWHM) pulse length focused to spot sizes varying from 25 – 100 μm (FWHM) diameter. This gave laser irradiances on target of between $8 \times 10^{17} \text{ W cm}^{-2}$ to $6 \times 10^{18} \text{ W cm}^{-2}$. The focal spot size was monitored with an x-ray pinhole camera. The CCD used was an EEV 05-30 model consisting of an 1152×1248 pixel array with each pixel having a $22.5 \times 22.5 \mu\text{m}^2$ dimension in a miniature, vacuum compatible camera head.⁷ The CCD signal was digitized by a low noise 16-bit 50 kHz analog to digital convertor (ADC). A light-tight filter of $\sim 1 \mu\text{m}$ Al was placed in front of the detector.

II. RESULTS

A. EXPERIMENTAL SPECTRA

Figure 1 shows two x-ray spectra of laser-heated 1 μm Al foils. The most intense spectral features are identified as the Al

^{a)}Contributed paper published as part of the Proceedings of the 19th Topical Conference on High-Temperature Plasma Diagnostics, Monterey, California, May, 2012.

^{b)}Author to whom correspondence should be addressed: dunn6@llnl.gov

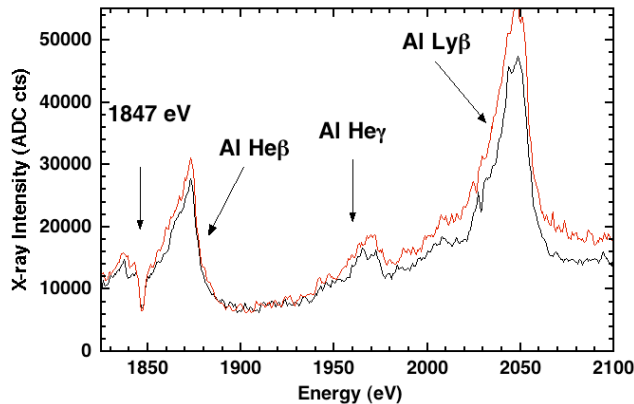


FIG. 1. Two laser plasma x-ray spectra from an Al foil target showing strong He-like and H-like lines recorded with a KAP (100) flat crystal spectrometer with a CCD detector. An absorption feature associated with the CCD is shown at 1847 eV.

He β line at 1869 eV, the He γ line at 1964 eV and the Ly β line at 2048 eV. The lines sit on a strong free-bound continuum. A second feature at 1847 eV in the low energy wing of the Al He β line is observed and is identified as a narrow absorption feature. The local x-ray intensity is reduced by $\sim 60\%$ in the dip. This absorption line was observed repeatedly in many shots at the same photon energy with different target materials and so was discounted as a plasma spectral feature. The absorption line was identified from the CCD, specifically as XAFS from SiO₂ material present in the electrode gate structure of this particular front-illuminated device. Both the type of material and thickness in the electrode acts as an absorbing layer reducing the quantum detection efficiency. Characterization of these materials would give detailed information about the device in use. However, the presence of strong emission lines as shown in Fig. 1 masks much of the detailed structure associated with the absorbing layers on the device. An intense, constant continuum spectrum is required.

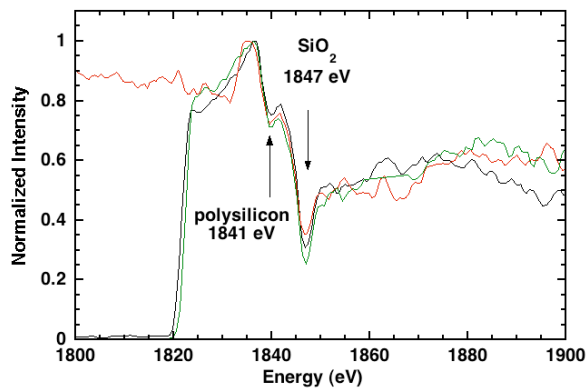


FIG. 2. Normalized continuum spectra for three shots from laser-heated CH targets. XAFS structure due to CCD electrode structure produces identified absorption features.

Figure 2 shows the emission spectra from a laser-produced plasma $\sim 12 \mu\text{m}$ thick CH foil target recorded on three separate shots. These targets were used to produce an intense continuum spectrum free of emission lines in the narrow 100 eV energy band centered on the Si K-edge at 1840 eV. A background image has been subtracted from the 2-dimensional spectral image, and the Al line calibration of Fig. 1 is used to produce the energy scale. The x-ray emission intensity varies on each shot and so for clarity, the spectrum has been normalized to the peak feature at the K-edge. Some noise and variation in the spectra at 1850 to

1900 eV is due to the presence of hard x-rays and suprathermal electrons detected by the CCD in random pixels. Two of the spectra are cut off below 1820 eV due to the spectrometer setting.

The change in the spectrometer linear energy dispersion dE/dx in this narrow energy range and shallow Bragg angles is small. Secondly, the variation in crystal integrated reflectivity for KAP (100) is very small (less than $\pm 1\%$) and is effectively flat based on measured and calculated values.^{8,9} The transmission of the $1 \mu\text{m}$ Al filter also varies by $\pm 5\%$ and is at the same level of the spectral differences. For these reasons, no further corrections were made to the data to correct for spectrometer response. The three spectra show remarkably similar features that match closely in energy position and intensity. These are the SiO₂ XAFS white line, clearly reproduced at 1847 eV, and the expected drop across the Si K-edge from 1820 to 1860 eV due to x-ray attenuation in the gate structure. This drop across the Si K-edge is strongly dependent on the total thickness of dead Si on the front of the CCD.^{1,3} The variation in the dioxide white line is due to changes in the laser focal spot size from shot to shot and the resultant effect on the flat crystal spectrometer resolution. Secondary features are also well reproduced including the smaller dip at 1841 eV due to the polysilicon gate absorption feature^{3,4} and the small peak observed at 1837 eV. The latter is associated with the combined effect of absorption in the epitaxial layer and the gate structure and will be discussed in the next sections.

B. QUANTUM DETECTION EFFICIENCY MODEL

Interpretation of the quantum detection efficiency from Figure 2 spectral measurements around the Si K-edge requires precise photo-absorption data for the materials in the epitaxial layer and the gate structure, specifically polysilicon Si, amorphous Si₃N₄ and amorphous SiO₂. The data sets available in the literature work well away from the K-edge structure but do not have the fine structure detail in the near edge vicinity. Measurements by Prigozhin et al.³ and Owens et al.⁴ using calibrated monochromatic x-rays from synchrotron sources have mapped out the absorption for known thin layers and sandwiches of these materials. The objective of this previous work was to better characterize the energy dependence and the strong effect on the absorption coefficients near the absorption edges. The absorption data was carefully selected, compared and extracted from these two works by digitizing the figures and converting to photo-absorption coefficients. This is particularly important for the dioxide white line feature that is very narrow and the

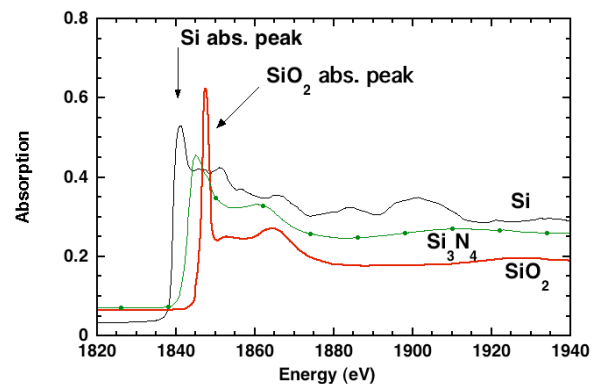


FIG. 3. X-ray absorption of $0.5 \mu\text{m}$ of polysilicon (black line), silicon dioxide (red thick line) and silicon nitride (green line with dots) at the Si K-edge. Absorption data based on measured results from ref. 3 and 4. (Color online)

dominant feature in Fig. 2. Figure 3 shows the different XAFS features in the narrow range of 1820 – 1940 eV for the gate electrode materials for 0.5 μm thickness. The absorption clearly shows the unique features and chemical shifts in the structure between 1830 eV and 1860 eV. Absorption fine structure oscillations in the polysilicon continue for several hundred electron volts above the Si K-edge. This is important to identifying and interpreting the features of Fig. 2 and applying the detection efficiency model. The QDE model developed in this work utilizes literature photo-absorption coefficients for the materials in the gate structure and epitaxial layer far away from the Si K-edge, for example,¹⁰ and uses the Prigozhin- and Owens-based data near the Si K-edge in fine energy bins. The model assumes area-averaged thicknesses with no detail in the geometrical electrode gate structure that in practice varies in thickness and materials across the array. The effect of angle of incidence of the x-rays relative to normal is included.

C. DATA FIT AND FINAL QDE CURVE

Figure 4 shows the QDE model comparison to the experimental data. The fit procedure is applied in several stages and converges to repeatable values for each layer. Good agreement is achieved on all of the spectral features described in section II.A. The nitride edge structure sits unresolved between the polysilicon and dioxide features but contributes to the absorption across the Si K-edge. The edge XAFS features allow the average electrode thickness to be determined to 1080 nm with each material thickness known to ± 50 nm. The height of the

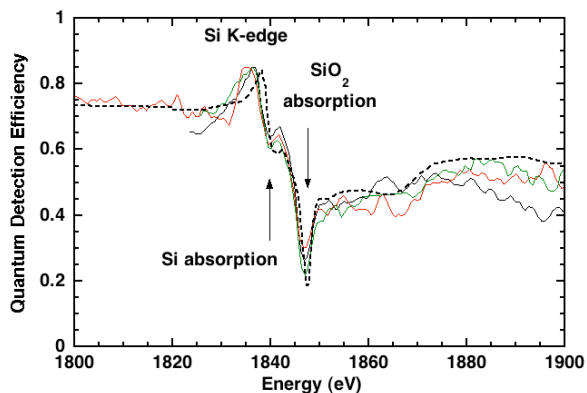


FIG. 4. Detection efficiency model (dashed line) applied to continuum spectrum of Fig. 2. Good agreement is found on all main observed spectral features. (Color online)

peak-spike (at ~ 1836 eV) as a ratio to the QDE at 1820 eV energy is sensitive to the epitaxial layer thickness. For this CCD, the detector active region is estimated to be $25 \pm 1 \mu\text{m}$.

Figure 5 shows the device QDE from 0.2 to 10 keV based on the model fit to the experimental continuum data. This curve agrees well with a similar EEV device reported previously with a high-resolution crystal spectrometer.¹¹ It can be seen that the QDE is highest above 85% at 3.5 keV with overall efficiency exceeding 50% over a broad energy range from 1 – 6 keV. The dioxide white line drops the efficiency to 20% at the Si K-edge. The QDE drops at the energy extremes for harder x-rays due to reduced absorption in the epitaxial layer and for energies below 1 keV due to absorption in the electrode structure. The characterization of the silicon, dioxide and nitride content in the

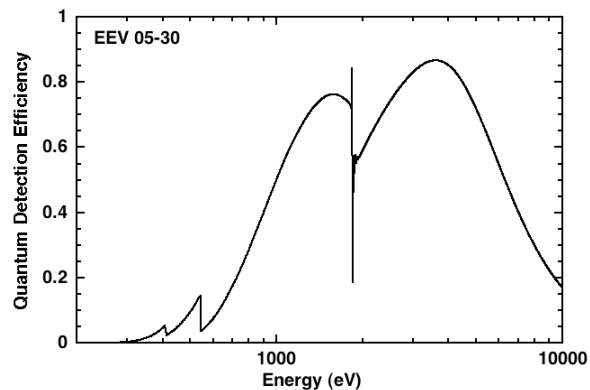


FIG. 5. Final quantum detection efficiency model for 0.2 to 10 keV photon energy range.

gate structure allows the fall in the expected efficiency to be predicted at lower energies.

IV. CONCLUSIONS

The calibration of a CCD detector has been reported using the CCD as part of a flat crystal wavelength dispersive spectrometer. The instrument measures the spectrum of a laser-produced continuum x-ray source in a narrow energy range. The study of the Si K-edge XAFS in the continuum spectrum due to the CCD electrode and epitaxial layer allows the precise determination of the type and thickness of absorbing dead layers. This leads to the determination of the absolute detector quantum efficiency. This simple but effective technique works well for a front-illuminated device but could also be applied to back-thinned devices and other pixelated solid-state detectors.

V. ACKNOWLEDGMENTS

The authors would like to thank David Hoarty of AWE and Ronnie Shepherd of LLNL for their useful discussions. This work performed under the auspices of the U.S. Department of Energy by Lawrence Livermore National Laboratory under Contract DE-AC52-07NA27344.

¹C. Castelli, A. Wells, K. McCarthy, and A. Holland, Nucl. Instrum and Methods in Phys. Res. A, **310**, 240 (1991).

²Yuelin Li, G.D. Tsakiris, and R. Sigel. Rev. Sci. Instrum., **66**, 80 (1995).

³G.Y. Prigozhin, J. Woo, J.A. Gregory, A.H. Loomis, M.W. Bautz, G.R. Ricker and S. Kraft, Opt. Eng., **37**, 2848 (1998).

⁴A. Owens, G.W. Fraser, and S.J. Gurman, Rad. Phys. and Chem., **65**, 109 (2002).

⁵J. L. Gaines and F. J. Wittmayer, SPIE Proc. **689**, 155 (1986).

⁶J. Dunn, A. D. Conder, and R.E. Stewart, SPIE proc. **3301**, 100 (1998).

⁷A. D. Conder, J. Dunn, and B. K. F Young, Rev. Sci. Instrum. **66**, 709 (1995).

⁸A. J. Burek, Space Sci. Inst. **2**, 53 (1976).

⁹M. Lewis, "A Quantitative Treatment of Bragg Diffraction", Ph. D Thesis, University of Leicester, UK (1982).

¹⁰B. L. Henke, E. M. Gullikson, and J. C. Davis, Atomic Data and Nuclear Data Tables **54**(2), 181-342 (1993); Photoabsorption coefficients generated from transmission data at Lawrence Berkeley National Laboratory, Center for X-ray Optics website at <http://www-cxro.lbl.gov/>

¹¹R. Barnsley, N. J. Peacock, J. Dunn, I. M. Melnick, I. H. Coffey, J. A. Rainnie, M. R. Tarbutt, and N. Nelms, Rev. Sci. Instrum. **74**, 2388 (2003).